

# High accuracy water potential energy surface for the calculation of infrared spectra

Irina I. Mizus, Aleksandra A. Kyuberis, Nikolai F. Zobov, Vladimir Yu. Makhnev

*Institute of Applied Physics, Russian Academy of Science,  
Ulyanov Street 46, Nizhny Novgorod, Russia 603950*

Oleg L. Polyansky, Jonathan Tennyson  
*Department of Physics and Astronomy,  
University College London, Gower Street,  
London WC1E 6BT, United Kingdom*

(Dated: September 18, 2018)

## Abstract

Transition intensities for small molecules such as water and CO<sub>2</sub> can now be computed with such high accuracy that they are being used to systematically replace measurements in standard databases. These calculations use high accuracy *ab initio* dipole moment surfaces and wavefunctions from spectroscopically-determined potential energy surfaces. Here an extra high accuracy potential energy surface (PES) of the water molecule (H<sub>2</sub><sup>16</sup>O) is produced starting from an *ab initio* PES which is then refined to empirical rovibrational energy levels. Variational nuclear motion calculations using this PES reproduce the fitted energy levels with a standard deviation of 0.011 cm<sup>-1</sup>, approximately three times their stated uncertainty. Use of wavefunctions computed with this refined PES is found to improve the predicted transition intensities for selected (problematic) transitions. A new room temperature line list for H<sub>2</sub><sup>16</sup>O is presented. It is suggested that the associated set of line intensities is the most accurate available to date for this species.

## I. INTRODUCTION

Most processes in chemical physics are governed by potential energy surfaces (PESs) and access to accurate PESs therefore allows the accurate prediction of properties. In a series of papers Murrell and co-workers developed analytic methods of representing PESs for small (usually triatomic) molecules [1] – [7]. Surfaces predicted on the basis of *ab initio* electronic structure calculations were usually improved by comparison with or fitting to spectroscopic data. This is precisely the technique we employ here. Much of this work on PESs is captured in the book “Molecular Potential Energy Functions” by Murrell *et al.* [8].

Water molecule is the number one molecule in the HITRAN database [9], which reflects its importance in the Earth’s atmosphere, and is a key constituent of other solar system bodies, exoplanets and cool stars [10]. It is therefore unsurprising that Sorbie and Murrell, in their seminal paper on constructing PESs, chose to concentrate on water [1]. Many other groups have subsequently followed their lead in constructing accurate semi-empirical PESs for water [11–16], the current authors included [17–22]. An important aspect of the study of the water molecule and the use of the results of these studies in the modelling of different terrestrial and astrophysical environments is the ability to accurately predict line intensities.

Over the last two decades, significant improvements have been made the accuracy of the water PESs; residuals in predicted rotation-vibration line positions have dropped from about  $0.6\text{ cm}^{-1}$  [17, 18] to  $0.025\text{ cm}^{-1}$  [15, 21]. However, still this figure is about an order-of-magnitude larger than the uncertainty in empirical determinations of rotation-vibration energy levels [23, 24]. Improving these predictions towards experimental accuracy places high significance on every step of the calculation. As demonstrated below, these improvements are important not only for accurately reproducing line positions, but also for the generation of accurate wavefunctions for use in intensity calculations.

A testimony to the improvement in the accuracy of computed infrared transition intensities based on the use of *ab initio* dipole moment surfaces (DMSs) is the systematic adoption of computed intensities in the place of measured one for both water and  $\text{CO}_2$  in the recent (2016) release of HITRAN [9]. Use of this methodology is particularly powerful for isotopically substituted species for which the accuracy of the computations is essentially unchanged [25–27], but experimental determinations become much harder. These studies employ the Lodi-Tennyson method [28] which uses stability analysis based on calculations using two

different PESs and two different DMSs to identify “unstable” transitions for which the computed intensities are not reliable. Significant differences between intensities calculated using different PESs for certain transitions have been found for water [27, 29], CO<sub>2</sub> [30] and H<sub>2</sub>CO [31]. Conversely, for many transitions it has proved possible to compute the line intensities for water [29, 32] and CO<sub>2</sub> [33] with sub-percent accuracy, which reflects the accuracy of the underlying *ab initio* DMS. To make further progress on this problem it becomes important to estimate and eliminate the causes of the remaining uncertainties. The largest of these appears to be the calculation of wavefunctions for states which are affected by accidental interactions with other states of the same overall symmetry; spectroscopists generally call these interactions resonances. It is the failure to precisely treat these resonances that leads to the unstable transitions. As shown below, better treatment can be achieved by systematic improvement of the PES and hence the wavefunctions.

Section II describes the procedure used to obtain our new PES. Section III presents the computed energy levels obtained using our new PES. Section IV compares and discusses calculations of intensities using different PESs. Section V describes our new, room temperature H<sub>2</sub><sup>16</sup>O line list. Section VI presents our conclusions and plans for further work.

## II. NEW POTENTIAL ENERGY SURFACE

As a starting point for the optimization process we used a semi-empirical PES due to Bubukina *et al.* [21]. Bubukina *et al.* in turn used the high quality CVRQD *ab initio* PES [34, 35] as their starting point and augmented this surface with corrections for adiabatic [36], relativistic [37], and quantum electrodynamics (QED) [38] effects. This fully *ab initio* starting point predicts rotation-vibration energy levels with an accuracy of about 1 cm<sup>-1</sup>.

### A. Nuclear motion calculation

Variational nuclear motion calculations were performed in Radau coordinates using DVR3D [39]. Morse-like oscillators with the values of parameters  $r_e = 2.55$ ,  $D_e = 0.25$  and  $\omega_e = 0.007$  in atomic units were used for both radial coordinates, and associated Legendre functions for the angular coordinate as basis functions. The corresponding discrete variable representation (DVR) grids contained 29, 29 and 40 points for these coordinates,

respectively. The final diagonalized vibrational matrices had a dimension of 1500. For the rotational problem, the dimensions of final matrices can be obtained as  $400(J + 1 - p)$ , where  $J$  is the total angular momentum quantum number and  $p$  is the value of parity. Only nuclear masses were used in these calculations. To ensure good accuracy for high- $J$  calculations, we followed Bubukina *et al.* [21]’s approach to rotational non-adiabatic effects which adopts a simplification [40] of *ab initio* procedure developed by Schwenke [41] for treating non-Born-Oppenheimer effects. The values of the adjustable parameters used by Bubukina *et al.* to scale Schwenke’s results were left unchanged.

## B. Optimization results

The optimization procedure was based on a method developed by Yurchenko *et al.* [42].

This method allows the fit to simultaneously optimize reproduction of empirical energy levels and *ab initio* grid points. This procedure helps the fit to avoid nonphysical behavior in the optimized PES. For this purpose we used a set of 677 *ab initio* energies computed by Grechko *et al.* [43] in the energy region up to  $25\,000\text{ cm}^{-1}$  (about 2.7% of *ab initio* points from the original set of 696 energies were excluded from the fit).

In the fit, we varied the values of 240 potential parameters of the starting PES to obtain the best predicts of the most-accurate available empirical energy levels [24]. As a result, we obtain a potential which reproduces the set of 847 empirical energy levels with  $J$  values 0, 2 and 5, and lying below  $15\,000\text{ cm}^{-1}$  with a standard deviation of  $0.011\text{ cm}^{-1}$ . The initial fit had the *ab initio* grid points weighted at  $10^{-4}$  the empirical data to ensure that PES remained physical, i.e. did not develop holes, in the region of interest. For the final stages of the fit this weighting was reduced to  $10^{-8}$ . About 3% of energy levels from the complete empirical set in the energy region of interest (26 from the total set of 873 energies) were excluded from the fit. Most of these levels (about 20) have high values of bending quantum number  $\nu_2$  and sample a region of the potential which is not well-characterized by fit. The standard deviation of our final PES with respect to the set of Born-Oppenheimer *ab initio* points is about  $68.8\text{ cm}^{-1}$ , a figure which depends strongly on high energy points.

Because the PES is designed for studies of states up to  $15\,000\text{ cm}^{-1}$  we refer to it as PES15k below. A Fortran program giving the PES15k potential is given in the supplementary material.

### III. RESULTS OF THE ENERGY LEVELS CALCULATIONS

Table I presents results of a  $J = 0$  calculations using PES15k.

Table II presents results of a comparison of the standard deviations for states with rotational quantum numbers  $J$  up to 15 and lying below  $15\,000\text{ cm}^{-1}$  using the PES of Bubukina *et al.* [21] and PES15k. These standard deviations are computed from the discrepancies between calculated and experimental levels as follows. Empirical energy levels up to  $J = 15$  were taken from the recent IUPAC compilation [24, 44]. Not all the levels were included for the comparison. Some of the levels - about 2% of those derived in [24] were excluded as they were outliers. There are two reasons that certain levels might show larger discrepancies. First, it could be the genuine experimental inaccuracy or incorrectly incorporated data. A number of problems with the IUPAC compilation of energy levels have been identified and are in the processes of being fixed [45]. Second, our model becomes worse for very highly excited  $\nu_2$  bending vibrational quantum numbers and correspondingly for very highly excited  $K_a$  rotational quantum numbers. There are particular issues with quantum numbers of high  $\nu_2$  states [46] and transitions to these states are in general much weaker than the other transitions, thus the influence of such lines on the accuracy of any line list is minor. As we can see from Table II, the improved average accuracy, expressed in the form of the standard deviation, varies between a factor of 1.5 to 2, which is significant.

### IV. COMPARISON OF INTENSITIES

The intensity of a transition depends on the square of the transition dipole. The transition dipole between two states can be computed using the expression:

$$\mu_{if} = \sum_t \langle i | \mu_t | f \rangle \quad (1)$$

where for a vibration-rotation transition, the initial and final states are represented by nuclear motion wave functions  $|i\rangle$  and  $|f\rangle$ , and the sum runs over the components of the internal dipole moment vector,  $\underline{\mu}$ . For a given DMS, differences in the values of the intensities reflect differences in the wavefunctions obtained as a result of the solution of the nuclear-motion Schrödinger equation for a certain PES. In this work all calculations use the LTP2011 DMS of Lodi *et al* [32], which is the most accurate DMS currently available.

TABLE I: Observed vibrational band origins below  $15\,000\text{ cm}^{-1}$  calculated with the new PES; values are in  $\text{cm}^{-1}$ .

$v_1v_2v_3$	obs	calc	obs-calc	$v_1v_2v_3$	obs	calc	obs-calc
0 1 0	1594.7463	1594.7523	0.0060	0 0 1	3755.9285	3755.9277	-0.0009
0 2 0	3151.6298	3151.6453	0.0155	0 1 1	5331.2673	5331.2658	-0.0015
1 0 0	3657.0533	3657.0406	-0.0126	0 2 1	6871.5202	6871.5225	0.0023
0 3 0	4666.7905	4666.7948	0.0043	1 0 1	7249.8169	7249.8175	0.0006
1 1 0	5234.9756	5234.9759	0.0004	0 3 1	8373.8514	8373.8529	0.0015
0 4 0	6134.0150	6134.0207	0.0057	1 1 1	8806.9990	8806.9972	-0.0018
1 2 0	6775.0935	6775.0906	-0.0029	0 4 1	9833.5829	9833.5805	-0.0025
2 0 0	7201.5399	7201.5414	0.0016	1 2 1	10328.7293	10328.7248	-0.0044
0 0 2	7445.0562	7445.0269	-0.0293	2 0 1	10613.3563	10613.3510	-0.0053
0 5 0	7542.3725	7542.4207	0.0482	0 0 3	11032.4041	11032.3939	-0.0102
1 3 0	8273.9757	8273.9713	-0.0044	0 5 1	11242.7757	11242.7716	-0.0041
2 1 0	8761.5816	8761.5851	0.0035	1 3 1	11813.2069	11813.2046	-0.0023
0 1 2	9000.1360	9000.1258	-0.0103	2 1 1	12151.2539	12151.2438	-0.0101
2 2 0	10284.3644	10284.3588	-0.0055	0 1 3	12565.0064	12564.9970	-0.0094
0 2 2	10521.7577	10521.7435	-0.0142	1 4 1	13256.1550	13256.1584	0.0034
3 0 0	10599.6860	10599.6789	-0.0071	2 2 1	13652.6532	13652.6523	-0.0009
1 0 2	10868.8747	10868.8608	-0.0139	3 0 1	13830.9368	13830.9336	-0.0032
2 3 0	11767.3890	11767.3673	-0.0217	0 2 3	14066.1936	14066.1769	-0.0167
0 3 2	12007.7743	12007.7778	0.0034	1 0 3	14318.8121	14318.8008	-0.0113
3 1 0	12139.3153	12139.3065	-0.0088	1 5 1	14647.9733	14647.9996	0.0263
1 1 2	12407.6620	12407.6465	-0.0155				
3 2 0	13640.7166	13640.6811	-0.0355				
4 0 0	13828.2747	13828.2615	-0.0132				
1 2 2	13910.8936	13910.8796	-0.0140				
2 0 2	14221.1585	14221.1459	-0.0126				
0 0 4	14537.5043	14537.4859	-0.0184				

TABLE II: Standard deviation, in  $\text{cm}^{-1}$ , as function of rotational excitation,  $J$ , of  $\text{H}_2^{16}\text{O}$  energy levels obtained from calculations with two PESs with respect to the empirical energy levels [24];  $N$  gives the number of levels considered for each  $J$ .

J	N	Bubukina <i>et al</i> [21]	PES15k
0	41	0.0145	0.0108
1	148	0.0181	0.0116
2	249	0.0239	0.0110
3	356	0.0186	0.0109
4	450	0.0166	0.0101
5	548	0.0174	0.0092
6	623	0.0169	0.0104
7	663	0.0162	0.0111
8	682	0.0238	0.0153
9	662	0.0257	0.0188
10	610	0.0280	0.0215
11	586	0.0328	0.0260
12	545	0.0400	0.0288
13	495	0.0432	0.0313
14	441	0.0483	0.0335
15	387	0.0491	0.0347

The steady improvement in intensity measurements [33, 47–50, 50, 51] towards the sub-percent level of accuracy has paralleled attempts to improve the accuracy of intensity calculations. Given an accurate, *ab initio* DMS [32, 33], the Lodi-Tennyson method [28] tests for unstable transitions, whose intensities can not be determined accurately. These transitions are identified on the basis of four line list calculations using two PESs and two DMSs. The usefulness of the Lodi-Tennyson method depends strongly on the accuracy of both the primary PES and the secondary PES. For example, attempts to use an *ab initio* PES as a secondary PES normally results in a significant overestimation of number of unstable lines [30]. Thus, we need extremely accurate PESs for at least three reasons. The first is determination of the most accurate line positions in the calculation of molecular line lists. The

TABLE III: Comparison of intensities computed using wavefunctions from the PES15k and Bubukina *et al* [21]. The comparison is for 8686 transitions between states with  $J \leq 4$ . The percentage differences are computed as  $100 \times (I(\text{PES15}) - I(\text{Bubukina})) / I(\text{PES15})$ .

%	number of lines
$\geq 20\%$	8
5%-20%	73
2%-5%	213
1%-2%	292
0.2% - 0.5%	1090
$\leq 0.1\%$	4974

second is for accurate wavefunctions which can be used for the accurate intensity calculations. The third is that an excellent pair of PESs are necessary for the Lodi-Tennyson-style evaluation of stability.

For these purposes it is important to evaluate what is the difference in intensity accuracy for the different lines using the same DMS and two different very accurate PESes. As it is shown in the previous section, the accuracy of the PES of this work is extremely high, whereas the accuracy of the PES of Bubukina *et al* [21] is also very high, it becomes an interesting problem to compare the intensities coming from these two PESes. For this purpose we computed linelist considering all transitions below 15 000  $\text{cm}^{-1}$  involving states with up to  $J = 4$  using these two PES. Table III presents a comparison of the differences in intensities of resulting 8701 lines. It can be seen that for most of the lines, more than 75 %, the transition intensity is essentially unchanged (changes by less than 0.1%) by the change wavefunctions, while approximately 1% of the lines change by more than 5%.

Table IV presents an example of the calculation of intensities of water absorption lines in the small spectra region between 3495 and 3500  $\text{cm}^{-1}$  using wavefunctions calculated by two different PESs: PES15k (this work) and Bubukina *et al* [21]. For many lines, the difference is less than 0.1 %. Some of the lines intensities differ more significantly by around 0.2 %. There are also a few lines with a significant difference in intensities of more than 1%. For one line the difference is 13 %; this line was previously deemed unstable using the Lodi-Tennyson method [29].



TABLE IV: Sample comparison of intensity calculations for the region  $3495 - 3500 \text{ cm}^{-1}$ . Experimental measurements are taken from Loos *et al.* [29, 52] and have uncertainties better than 1%. The predicted intensities used wavefunctions calculated using PES15k (this work) and the PES of Bubukina *et al* [21].

Frequency	Assignment	$I(\text{exp})$	$I(\text{PES15k})$	$I(\text{Bubukina})$	$\delta I(\text{PES15k})/\%$	$\delta I(\text{Bubukina})/\%$
3495.065	1 0 0 13 3 10 0 0 0 13 4 9	2.62(-25)	2.6063(-25)	2.6054(-25)	-0.45	-0.48
3495.176	1 0 0 6 2 5 0 0 0 7 1 6	1.62(-21)	1.6070(-21)	1.6086(-21)	-0.93	-0.83
3495.506	1 0 0 13 5 8 0 0 0 14 4 11	1.44(-25)	1.4901(-25)	1.4904(-25)	3.36	3.38
3496.164	1 1 0 2 1 2 0 1 0 3 2 1	1.51(-24)	1.4784(-24)	1.4776(-24)	-2.07	-2.12
3496.279	1 0 0 9 4 6 0 0 0 9 5 5	9.76(-24)	9.6424(-24)	9.6300(-24)	-1.25	-1.38
3496.383	1 0 0 11 5 6 0 0 0 12 4 9	6.21(-24)	6.1797(-24)	6.1846(-24)	-0.54	-0.46
3496.624	1 0 0 5 1 4 0 0 0 6 2 5	3.30(-21)	3.2581(-21)	3.2555(-21)	-1.28	-1.37
3496.917	1 0 0 11 7 5 0 0 0 12 6 6	3.73(-25)	3.7945(-25)	3.8019(-25)	1.75	1.94
3497.601	0 2 0 5 5 0 0 0 0 6 2 5	2.29(-23)	2.1521(-23)	2.4768(-23)	-6.27	7.66
3497.985	1 0 0 10 6 5 0 0 0 11 5 6	1.29(-23)	1.2870(-23)	1.2898(-23)	0.00	0.22
3498.602	0 0 1 6 3 4 0 0 0 6 5 1	6.70(-23)	6.6933(-23)	6.7045(-23)	-0.06	0.11
3499.420	1 1 0 6 3 4 0 1 0 6 4 3	1.58(-25)	1.5306(-25)	1.5297(-25)	-3.03	-3.09
3499.561	0 0 1 15 3 13 0 0 0 15 3 12	7.71(-26)	7.5541(-26)	7.5730(-26)	-2.00	-1.74
3499.746	0 0 1 8 5 3 0 0 0 9 5 4	7.79(-22)	7.8226(-22)	7.8306(-22)	0.47	0.57
3499.925	0 2 0 7 3 4 0 0 0 6 2 5	8.07(-23)	8.1491(-23)	8.1537(-23)	0.99	1.05

Figure 1 gives a similar comparison with the recent high accuracy measurements of Sironneau and Hodges [50] who consider 70 unblended water lines in the transparency window region from  $7710$  to  $7920 \text{ cm}^{-1}$ ; the stated uncertainty of these measurements is only 0.20%. For most transitions the difference between the predictions of calculations performed with wavefunctions from the PES15k and Bubukina *et al.* PESs is small. However, in general our new calculations with PES15k give results closer to the measurements.

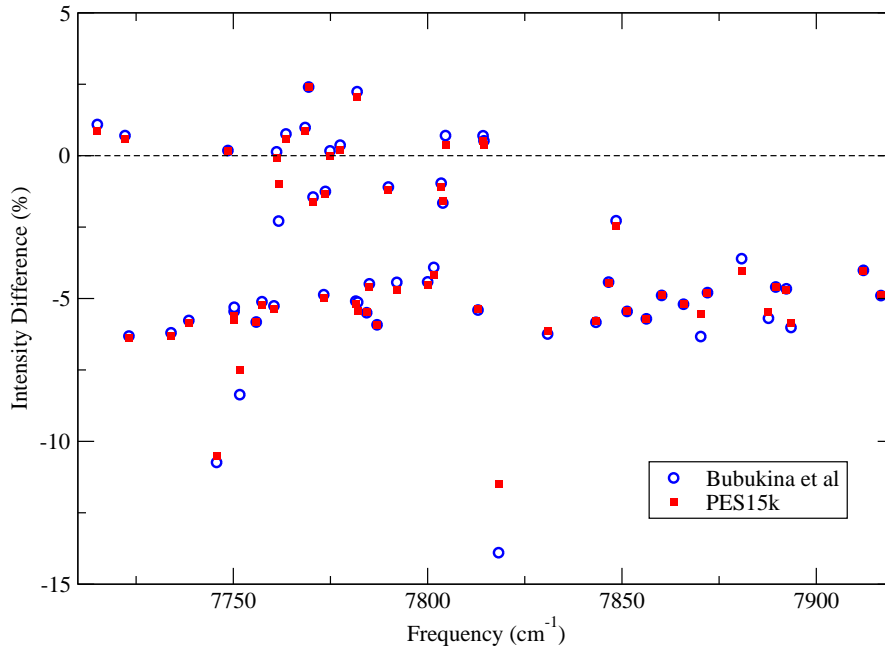


FIG. 1: Differences, percent of the observed value, for transition intensities predicted using wavefunctions from the PES15k and Bubukina *et al.* [21]. The observed data is taken from the recent high accuracy measurements by Sironneau and Hodges [50].

## V. LINE LIST CALCULATION

Given the improved quality of the intensities generated with the new PES15k potential, we have computed a new room temperature line list for  $\text{H}_2^{16}\text{O}$ . The line list uses the PES15k PES and the LTP2011 DMS [32]. The line list includes all transitions with an intensity greater than  $10^{29}$  cm/molecule at 296 K involving states with  $J \leq 15$  and transitions wavenumbers below 18 000  $\text{cm}^{-1}$ . This line list, which follows the HITRAN convention which scales the intensities to natural abundance, contains 132 034 transitions. It is given in HITRAN format as part of the supplementary data.

## VI. CONCLUSIONS

Since the pioneering work of Murrell and his group on the representation of potential energy surfaces for polyatomic molecules, the story has been one of steady improvement. The best surfaces are now capable of giving predictions competitive with spectroscopic measurements [53]. Of course a PES only exists within the Born-Oppenheimer approximation so the

generation of high accuracy potentials necessary brings beyond Born-Oppenheimer effects into play. How best to include these is a subject of active research for small molecules such as water [41, 54, 55].

There has been much recent emphasis on using highly accurate PES and *ab initio* DMS to compute transition intensities with accuracies approaching that achieved by many experimental studies. Understandably, much emphasis has been placed on *ab initio* techniques for computing high accuracy DMS [32, 56, 57]. However, the PES used plays an important role in providing reliable wavefunctions; this is particularly important for those states which are sensitive to interactions with other nearby states of the same overall  $J$  and symmetry. In this work we provide a new PES of improved accuracy which is used to provide a new H<sub>2</sub><sup>16</sup>O line list. We show that while for the majority of transitions use of wavefunctions generated employing this new PES simply replicate results already available; for a minority of transitions the use of the new PES gives results which are significantly different and which generally represent an improvement.

Our analysis shows that for more than 10% of the lines use of our improved PES results in a change in the predicted intensity by more than 0.1 %. Given that the most recent studies measure intensities for a few, carefully chosen H<sub>2</sub><sup>16</sup>O lines with an accuracy of 0.2% [50], improvements of this magnitude are important for the matching theoretical model. However, as is clear from the results presented above and from other published studies [29, 58], the best currently available *ab initio* DMS is not able to provide this level of for many bands. Work on improving the accuracy and extending the range of DMS is currently in progress.

### Acknowledgement

We thank Sergey Yurchenko for helpful discussions during the course of this work, This work was supported by the UK Natural Environment Research Council through grant NE/N001508/1 and the Russian Fund for Fundamental Studies.

---

[1] K. S. Sorbie and J. N. Murrell, Mol. Phys. **29**, 1387 (1975).

[2] J. N. Murrell, K. S. Sorbie, and A. J. C. Varandas, Mol. Phys. **32**, 1359 (1976).

- [3] S. Farantos, E. C. Leisegang, J. N. Murrell, K. Sorbie, J. J. C. Texeiradas, and A. J. C. Varandas, *Mol. Phys.* **34**, 947 (1977).
- [4] J. N. Murrell, S. Carter, and A. J. C. Varandas, *Mol. Phys.* **35**, 1325 (1978).
- [5] J. N. Murrell, S. Carter, I. M. Mills, and M. F. Guest, *Mol. Phys.* **37**, 1199 (1979a).
- [6] J. N. Murrell, S. Carter, and I. M. Mills, *Mol. Phys.* **37**, 1885 (1979b).
- [7] X. H. Liu and J. N. Murrell, *J. Chem. Soc., Faraday Trans.* **88**, 1503 (1992).
- [8] J. N. Murrell, S. Carter, S. C. Farantos, P. Huxley, and A. J. C. Varandas, *Molecular Potential Energy Functions* (John Wiley & Sons, Chichester, UK, 1984).
- [9] I. E. Gordon, L. S. Rothman, Y. Babikov, A. Barbe, D. C. Benner, P. F. Bernath, M. Birk, L. Bizzocchi, V. Boudon, L. R. Brown, et al., *J. Quant. Spectrosc. Radiat. Transf.* **203**, 3 (2017).
- [10] P. F. Bernath, *Int. Rev. Phys. Chem.* **28**, 681 (2009).
- [11] J. N. Murrell, S. Carter, I. M. Mills, and M. F. Guest, *Mol. Phys.* **42**, 605 (1981).
- [12] S. Carter and N. C. Handy, *J. Chem. Phys.* **87**, 4294 (1987).
- [13] L. Halonen and T. Carrington Jr., *J. Chem. Phys.* **88**, 4171 (1988).
- [14] C. D. Paulse and J. Tennyson, *J. Mol. Spectrosc.* **168**, 313 (1994).
- [15] H. Partridge and D. W. Schwenke, *J. Chem. Phys.* **106**, 4618 (1997).
- [16] S. N. Yurchenko, B. A. Voronin, R. N. Tolchenov, N. Doss, O. V. Naumenko, W. Thiel, and J. Tennyson, *J. Chem. Phys.* **128**, 044312 (2008).
- [17] O. L. Polyansky, P. Jensen, and J. Tennyson, *J. Chem. Phys.* **101**, 7651 (1994).
- [18] O. L. Polyansky, P. Jensen, and J. Tennyson, *J. Chem. Phys.* **105**, 6490 (1996).
- [19] J. S. Kain, O. L. Polyansky, and J. Tennyson, *Chem. Phys. Lett.* **317**, 365 (2000).
- [20] S. V. Shirin, O. L. Polyansky, N. F. Zobov, R. I. Ovsyannikov, A. G. Császár, and J. Tennyson, *J. Mol. Spectrosc.* **236**, 216 (2006).
- [21] I. I. Bubukina, O. L. Polyansky, N. F. Zobov, and S. N. Yurchenko, *Optics and Spectroscopy* **110**, 160 (2011).
- [22] O. L. Polyansky, N. F. Zobov, I. I. Mizus, L. Lodi, S. N. Yurchenko, J. Tennyson, A. G. Császár, and O. V. Boyarkin, *Phil. Trans. Royal Soc. London A* **370**, 2728 (2012).
- [23] J. Tennyson, N. F. Zobov, R. Williamson, O. L. Polyansky, and P. F. Bernath, *J. Phys. Chem. Ref. Data* **30**, 735 (2001).
- [24] J. Tennyson, P. F. Bernath, L. R. Brown, A. Campargue, M. R. Carleer, A. G. Császár,

- L. Daumont, R. R. Gamache, J. T. Hodges, O. V. Naumenko, et al., *J. Quant. Spectrosc. Radiat. Transf.* **117**, 29 (2013).
- [25] E. J. Zak, J. Tennyson, O. L. Polyansky, L. Lodi, N. F. Zobov, S. A. Tashkun, and V. I. Perevalov, *J. Quant. Spectrosc. Radiat. Transf.* **189**, 267 (2017).
- [26] E. J. Zak, J. Tennyson, O. L. Polyansky, L. Lodi, N. F. Zobov, S. A. Tashkun, and V. I. Perevalov, *J. Quant. Spectrosc. Radiat. Transf.* **203**, 265 (2017).
- [27] A. A. Kyuberis, N. F. Zobov, O. V. Naumenko, B. A. Voronin, O. L. Polyansky, L. Lodi, A. Liu, S.-M. Hu, and J. Tennyson, *J. Quant. Spectrosc. Radiat. Transf.* **203**, 175 (2017).
- [28] L. Lodi and J. Tennyson, *J. Quant. Spectrosc. Radiat. Transf.* **113**, 850 (2012).
- [29] M. Birk, G. Wagner, J. Loos, L. Lodi, O. L. Polyansky, A. A. Kyuberis, N. F. Zobov, and J. Tennyson, *J. Quant. Spectrosc. Radiat. Transf.* **203**, 88 (2017).
- [30] E. Zak, J. Tennyson, O. L. Polyansky, L. Lodi, S. A. Tashkun, and V. I. Perevalov, *J. Quant. Spectrosc. Radiat. Transf.* **177**, 31 (2016).
- [31] A. F. Al-Refaie, S. N. Yurchenko, A. Yachmenev, and J. Tennyson, *Mon. Not. R. Astron. Soc.* **448**, 1704 (2015).
- [32] L. Lodi, J. Tennyson, and O. L. Polyansky, *J. Chem. Phys.* **135**, 034113 (2011).
- [33] O. L. Polyansky, K. Bielska, M. Ghysels, L. Lodi, N. F. Zobov, J. T. Hodges, and J. Tennyson, *Phys. Rev. Lett.* **114**, 243001 (2015).
- [34] O. L. Polyansky, A. G. Császár, S. V. Shirin, N. F. Zobov, P. Barletta, J. Tennyson, D. W. Schwenke, and P. J. Knowles, *Science* **299**, 539 (2003).
- [35] P. Barletta, S. V. Shirin, N. F. Zobov, O. L. Polyansky, J. Tennyson, E. F. Valeev, and A. G. Császár, *J. Chem. Phys.* **125**, 204307 (2006).
- [36] J. Tennyson, *J. Phys. B: At. Mol. Opt. Phys.* **29**, 1817 (1996).
- [37] H. M. Quiney, P. Barletta, G. Tarczay, A. G. Császár, O. L. Polyansky, and J. Tennyson, *Chem. Phys. Lett.* **344**, 413 (2001).
- [38] P. Pyykkö, K. G. Dyall, A. G. Császár, G. Tarczay, O. L. Polyansky, and J. Tennyson, *Phys. Rev. A* **63**, 024502 (2001).
- [39] J. Tennyson, M. A. Kostin, P. Barletta, G. J. Harris, O. L. Polyansky, J. Ramanlal, and N. F. Zobov, *Comput. Phys. Commun.* **163**, 85 (2004).
- [40] J. Tennyson, P. Barletta, M. A. Kostin, O. L. Polyansky, and N. F. Zobov, *Spectrochimica Acta A* **58**, 663 (2002).

- [41] D. W. Schwenke, *J. Chem. Phys.* **118**, 10431 (2003).
- [42] S. N. Yurchenko, M. Carvajal, P. Jensen, F. Herregodts, and T. R. Huet, *Chem. Phys.* **290**, 59 (2003).
- [43] M. Grechko, O. V. Boyarkin, T. R. Rizzo, P. Maksyutenko, N. F. Zobov, S. Shirin, L. Lodi, J. Tennyson, A. G. Császár, and O. L. Polyansky, *J. Chem. Phys.* **131**, 221105 (2009).
- [44] J. Tennyson, P. F. Bernath, L. R. Brown, A. Campargue, A. G. Császár, L. Daumont, R. R. Gamache, J. T. Hodges, O. V. Naumenko, O. L. Polyansky, et al., *Pure Appl. Chem.* **86**, 71 (2014).
- [45] T. Furtenbacher, N. Dénes, J. Tennyson, O. V. Naumenko, O. L. Polyansky, N. F. Zobov, and A. G. Császár, *J. Quant. Spectrosc. Radiat. Transf.* (2017), (in preparation).
- [46] M. S. Child, T. Weston, and J. Tennyson, *Mol. Phys.* **96**, 371 (1999).
- [47] J. T. Hodges, D. Lisak, N. Lavrentieva, A. Bykov, L. Sinitsa, J. Tennyson, R. J. Barber, and R. N. Tolchenov, *J. Mol. Spectrosc.* **249**, 86 (2008).
- [48] G. Wuebbeler, G. J. P. Viquez, K. Jousten, O. Werhahn, and C. Elster, *J. Chem. Phys.* **135**, 204304 (2011).
- [49] M. Ghysels, Q. Liu, A. J. Fleisher, and J. T. Hodges, *Appl. Phys. B-Lasers Opt.* **123**, 124 (2017).
- [50] V. T. Sironneau and J. T. Hodges, *J. Quant. Spectrosc. Radiat. Transf.* **152**, 1 (2015).
- [51] T. Odintsova, E. Fasci, L. Moretti, E. J. Zak, O. L. Polyansky, J. Tennyson, L. Gianfrani, and A. Castrillo, *J. Chem. Phys.* **146**, 244309 (2017).
- [52] J. Loos, M. Birk, and G. Wagner, *J. Quant. Spectrosc. Radiat. Transf.* p. (in press) (2017).
- [53] M. Pavanello, L. Adamowicz, A. Alijah, N. F. Zobov, I. I. Mizus, O. L. Polyansky, J. Tennyson, T. Szidarovszky, A. G. Császár, M. Berg, et al., *Phys. Rev. Lett.* **108**, 023002 (2012).
- [54] L. G. Diniz, J. R. Mohallem, A. Alijah, M. Pavanello, L. Adamowicz, O. L. Polyansky, and J. Tennyson, *Phys. Rev. A* **88**, 032506 (2013).
- [55] A. Scherrer, F. Agostini, D. Sebastiani, E. K. U. Gross, and R. Vuilleumier, *Phys. Rev. X* **7**, 031035 (2017).
- [56] L. Lodi, R. N. Tolchenov, J. Tennyson, A. E. Lynas-Gray, S. V. Shirin, N. F. Zobov, O. L. Polyansky, A. G. Császár, J. van Stralen, and L. Visscher, *J. Chem. Phys.* **128**, 044304 (2008).
- [57] D. W. Schwenke and H. Partridge, *J. Chem. Phys.* **113**, 6592 (2000).
- [58] J. Lampel, D. Pöhler, O. L. Polyansky, A. A. Kyuberis, N. F. Zobov, J. Tennyson, L. Lodi,

U. Frieß, Y. Wang, S. Beirle, et al., *Atmos. Chem. Phys.* **17**, 1271 (2017).